

Revealing degree distribution of bursting neuron networks

Yu Shen, Zhonghuai Hou, and Houwen Xin

Citation: *Chaos: An Interdisciplinary Journal of Nonlinear Science* **20**, 013110 (2010); doi: 10.1063/1.3300019

View online: <http://dx.doi.org/10.1063/1.3300019>

View Table of Contents: <http://scitation.aip.org/content/aip/journal/chaos/20/1?ver=pdfcov>

Published by the [AIP Publishing](#)

Articles you may be interested in

[Intermittent synchronization in a network of bursting neurons](#)

Chaos **21**, 033125 (2011); 10.1063/1.3633078

[Chaotic phase synchronization in small-world networks of bursting neurons](#)

Chaos **21**, 013127 (2011); 10.1063/1.3565027

[Mesoscale and clusters of synchrony in networks of bursting neurons](#)

Chaos **21**, 016106 (2011); 10.1063/1.3563581

[Burst synchronization transitions in a neuronal network of subnetworks](#)

Chaos **21**, 016110 (2011); 10.1063/1.3559136

[Simulating Evoked Gamma Oscillations of Human EEG in a Network of Spiking Neurons Reveals an Early Mechanism of Memory Matching](#)

AIP Conf. Proc. **913**, 215 (2007); 10.1063/1.2746750



Revealing degree distribution of bursting neuron networks

Yu Shen,¹ Zhonghuai Hou,^{1,2,a)} and Houwen Xin¹

¹Department of Chemical Physics, University of Science and Technology of China, Hefei, Anhui 230026, People's Republic of China

²Hefei National Lab of Physical Science at Microscale, University of Science and Technology of China, Hefei, Anhui 230026, People's Republic of China

(Received 27 September 2009; accepted 7 January 2010; published online 8 March 2010)

We present a method to infer the degree distribution of a bursting neuron network from its dynamics. Burst synchronization (BS) of coupled Morris–Lecar neurons has been studied under the weak coupling condition. In the BS state, all the neurons start and end bursting almost simultaneously, while the spikes inside the burst are incoherent among the neurons. Interestingly, we find that the spike amplitude of a given neuron shows an excellent linear relationship with its degree, which makes it possible to estimate the degree distribution of the network by simple statistics of the spike amplitudes. We demonstrate the validity of this scheme on scale-free as well as small-world networks. The underlying mechanism of such a method is also briefly discussed. © 2010 American Institute of Physics. [doi:10.1063/1.3300019]

The relationship between the topology and dynamics on complex networks has been an intriguing and interesting topic in recent decades.^{1,2} On the other hand, the phenomena of spike and burst are of particular importance in the neuronal system. A lot of models have been proposed to understand the inner mechanisms and dynamical behaviors of spiking and bursting neurons.^{3,4} However, how the topology of a neuron network would influence its spiking or bursting activity is still an open question. In this article, we have studied the collective behavior of an ensemble of coupled Morris–Lecar (ML) neurons. We found that when the neurons are burst synchronized, the spiking amplitude of a given neuron is linearly dependent on its degree. Such a nice property provides us a useful way to derive the degree distribution of a bursting neuron network from its bursting activities.

In the past decade, the physics of network has gained great research attention^{1,2} ever since the pioneer work of Watts and Strogatz⁵ about the collective properties of small-world networks and that of Albert and Barabási⁶ about the emergence of scale-free degree distribution in many real-world networks. A central issue of this interdisciplinary science has been how the network topology would influence the dynamics taking place on it.⁷ For instance, synchronization of coupled chaotic oscillators is usually much easier on small-world or scale-free networks than on a regular one,⁸ epidemic thresholds are absent on scale-free networks,⁹ spatiotemporal chaos can be tamed by random shortcuts on small-world networks,¹⁰ to list just a few. For many real systems, such as networks of neurons, interacting proteins or genes, however, important aspects of the network structure are largely unknown. Therefore, “reverse engineering” methods to probe the network topology by studying various dy-

namic behaviors prove to be very useful and have gained growing attention recently.^{11–14} Yu *et al.*¹¹ developed an analytical and numerical approach to estimate the topology of a network based on the dynamic evolution on it. Arenas *et al.*¹² found that the transition process to synchronization can be used to detect the community structure in a hierarchical network. Timme¹³ showed that one can recover the topology of a coupled oscillator network by investigating its response to local stimulations. Bu *et al.*¹⁴ demonstrated that one can robustly estimate the degree distribution of coupled chaotic oscillator networks via analysis of the time series. These works have opened many perspectives in this direction and developments of new methods applied to real systems are still interesting and of ubiquitous importance.

In our previous work,¹⁵ we have studied the transition from spatiotemporal chaos to burst synchronization (BS) of coupled Hindmarsh–Rose (HR) neurons on small-world networks. We found “more degree, more spikes per burst” and two transition mechanisms (“spike adding” and “change in bursting type”) between different types of BS patterns. These results indicate that a neuron’s degree plays a very important role on its dynamics. Thus a very interesting question comes to us: can we use this kind of relationship between the degree and dynamics of a given neuron to perform reverse engineering, i.e., revealing degree distribution of a given neuron network from the dynamics?

However, we find that the answer to this question is not trivial. Actually we failed to deduce the degree distribution of a HR network from its BS behavior. After a detailed investigation, we figured out that the failure is mainly due to the nonstationarity of the HR neuron in the spiking zone, i.e., a neuron with more degree may attain more spikes through dual pathways, one via spike adding and the other via bifurcation from fold-homoclinic (FHC) bursting to fold-Hopf (FH) bursting. Therefore, we turn to ML model in the present work, where the intrabursting behavior is more stationary. Similar to the HR model, the ML neurons can also reach BS state under the weak-coupling condition, where all the neu-

^{a)}Author to whom correspondence should be addressed. Electronic mail: hzhlj@ustc.edu.cn.

rons start and end bursting almost simultaneously.¹⁶ In the BS state, the bursting properties of a given neuron, such as the number of spikes per burst, the bursting period, and the spike amplitude A_{spike} of a given neuron, are shown to be mainly dependent on its degree k . Interestingly, we find that A_{spike} is an excellent decreasing linear function of k , i.e., the more neighbors a neuron has, the smaller its spike amplitude is. Such a linear relationship makes it possible to estimate the network's degree distribution by simply investigating the distribution of A_{spike} . Since real neuron networks often have complex topology,¹⁷ we have demonstrated the validity of our scheme in scale-free networks with different scaling exponents γ as well as in small-world networks. We would like to emphasize here that the present work addresses a different problem as that in Ref. 15, i.e., revealing topology of a network from its dynamics, and the linear relationship between the degree and spike amplitude is a novel phenomenon that was not observed in the coupled HR networks.¹⁵

The ML model is a simplified version of the Hodgkin–Huxley model which describes the spiking and refractory properties of real neurons. For a single neuron, the transmembrane current is composed of the voltage-gated calcium (Ca^{2+}) and potassium (K^+) currents, the leaky current and a slowly adapted external current. The diffusively coupled ML models can be written as

$$C \frac{dV_i}{dt} = g_{\text{Ca}} m_{\infty}(V_i)(V_{\text{Ca}} - V_i) + g_{\text{K}} \omega_i(V_{\text{K}} - V_i) + g_l(V_l - V_i) + I_i + \varepsilon \sum_{j \in \Omega(i)} (V_j - V_i),$$

$$\frac{d\omega_i}{dt} = \lambda_{\infty}(V_i)(\omega_{\infty}(V_i) - \omega_i),$$

$$\frac{dI_i}{dt} = -\mu \left(\frac{1}{5} + V_i \right),$$

where $i=1, 2, \dots, N$ (N is the total number of neurons) and

$$m_{\infty}(V) = 0.5 \left(1 + \tanh \left(\frac{V - V_a}{V_b} \right) \right),$$

$$\omega_{\infty}(V) = 0.5 \left(1 + \tanh \left(\frac{V - V_c}{V_d} \right) \right),$$

$$\lambda_{\infty}(V) = \frac{1}{3} \cosh \left(\frac{V - V_c}{2V_d} \right).$$

Herein, V_i , ω_i , and I_i denote the transmembrane action potential, the activation of the K^+ current, and the external stimulus current of neuron i , respectively. $\mu=0.005$ is a small parameter which makes the time scale of I much lower than that of V or ω . The system parameters V_{Ca} , V_{K} , and V_l represent equilibrium potentials of Ca^{2+} , K^+ , and leak currents, respectively, and g_{Ca} , g_{K} , and g_l denote the maximum conductance of corresponding ionic currents. The last term in the first line of Eq. (1) represents the interaction between neurons with coupling strength ε , where the summation of j runs over the neighbors of neuron i denoted by $\Omega(i)$. The parameter set we used in our simulation is $C=1 \mu\text{F cm}^{-2}$, $g_{\text{Ca}}=1.2 \text{ mS cm}^{-2}$, $g_{\text{K}}=2.0 \text{ mS cm}^{-2}$, $g_l=0.5 \text{ mS cm}^{-2}$,

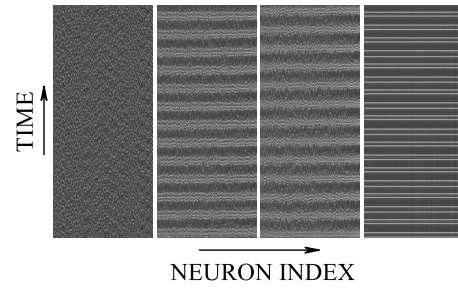


FIG. 1. Transition from spatiotemporal chaos (left panel) to BS (middle panels) and then to complete synchronous (right panel) on coupled scale-free ML networks with $N=400$ and $\gamma=3$. From left to right, the coupling strength is 0, 0.004, 0.005, and 0.5, respectively.

$V_{\text{Ca}}=0.84 \text{ mV}$, $V_{\text{K}}=-1.1 \text{ mV}$, $V_l=-0.5 \text{ mV}$, $V_a=-0.01 \text{ mV}$, $V_b=0.15 \text{ mV}$, $V_c=0.1 \text{ mV}$, and $V_d=0.05 \text{ mV}$. For a detailed explanation of the parameters, please see Ref. 18.

Many coupled neuron systems experience a (some) spatiotemporal ordered bursting synchronized state(s) before they are fully synchronized with increasing coupling strength or number of random links on complex networks.^{15,19–21} In Fig. 1, we show the spatiotemporal behavior of $V_i(t)$ on a scale-free network, generated by assigning degrees randomly to the network nodes according to the power law distribution $p(k) \sim k^{-\gamma}$, with $N=400$ and $\gamma=3$ for four increasing coupling strengths. Different gray levels correspond to different values of the action potential, i.e., $V_i(t)$ is larger in the brighter region. In the absence of coupling, each neuron is chaotic and the pattern is irregular. In the presence of a rather weak coupling, for instance, $\varepsilon=0.004$ and 0.005 , an ordered BS state can be observed. In this state, each neuron shows a rather regular bursting behavior in time, as shown in Fig. 2, where the action potential alternates, on a slow time scale, between a quiescent state and fast repetitive spiking. In addition, bursts start and end almost simultaneously throughout the network, while spikes inside the bursts are incoherent among the neurons. The BS pattern is almost periodic in time, and the period represents the time scale of the burst. With increasing coupling strength, spike coherence between the neurons is enhanced and the system finally reaches a complete chaotic synchronization when ε is large enough. We note here that the transition from spatiotemporal chaos to ordered BS state has also been observed in coupled network

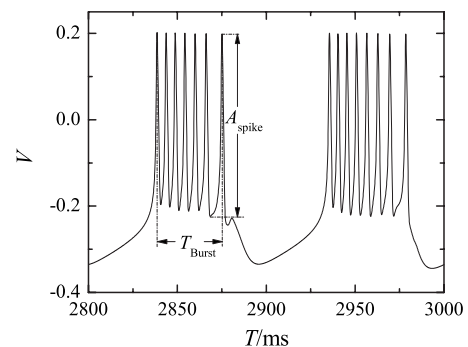


FIG. 2. Bursting behavior of a neuron in the BS state is shown. Two bursts with different number of spikes N_{SPB} are presented. The spike amplitude A_{spike} and bursting period T_{burst} are labeled.

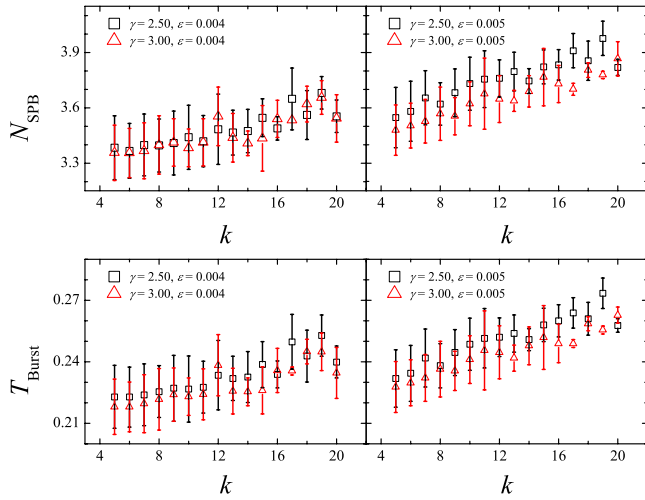


FIG. 3. (Color online) Number of spikes per burst and bursting period presented as functions of the neuron degree k for two different scale-free networks and two coupling strengths for each network.

of neurons described by HR model^{15,19} and a two-dimensional coupled-map-lattice model,²¹ and it was shown to be relevant with the mechanism of the central pattern generator.

As shown in Fig. 2, a burst can be characterized by the average spiking amplitude A_{spike} , the bursting period T_{burst} , and the number of spikes inside a burst N_{SPB} . A_{spike} is calculated as an average difference between successive local minima and maxima inside a burst. We are interested in how these properties of a given neuron depend on its degree k . In Fig. 3, we find that both N_{SPB} and T_{burst} increase with k , indicating that a neuron with larger degree will have more spikes inside a burst and longer burst duration. Coupling strength also plays a strong role and both quantities increase with it. The network topology does not matter much. Figure 4(a) shows the relationships between A_{spike} and k for different γ and ϵ . Interestingly, they are excellent decreasing linear functions, hence a neuron with more neighbors will have a smaller spike amplitude. Again, the data for different γ nearly collapse, while those for different ϵ do not. The slopes

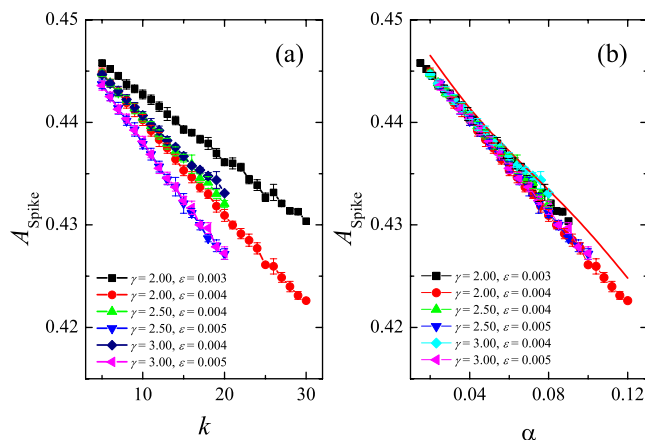


FIG. 4. (Color online) (a) Dependences of the spike amplitudes and neuron's degree on scale-free networks with different γ and ϵ . (b) Spike amplitude presented as a function of $\alpha = \epsilon k$ obtained from the simulation data in (a) (symbols) and the perturbed Eq. (4) (line).

of the linear fits seem to be proportional to the coupling strength. We draw A_{spike} as a function of $\alpha = \epsilon k$ in Fig. 4(b), and all the data in Fig. 4(a) collapse very well to a single straight line. A linear fit gives

$$A_i = A_0 - c\epsilon k_i \quad (2)$$

with $A_0 \approx 0.447$ and $c \approx 0.2$.

To get a qualitative understanding of the above linear relationship between A and α , we may write the first line in Eq. (1) in the form

$$C \frac{dV_i}{dt} = F(V_i, \omega_i, I_i) + \epsilon k_i (\bar{V}_i - V_i), \quad (3)$$

where $F(V_i, \omega_i, I_i) = g_{\text{Ca}} m_{\infty}(V_i)(V_{\text{Ca}} - V_i) + g_{\text{K}} \omega_i (V_{\text{K}} - V_i) + g_{\text{I}} (V_{\text{I}} - V_i) + I_i$, k_i is the degree of neuron i , and $\bar{V}_i = (1/k_i) \sum_{j \in \Omega(i)} V_j$ defines a local mean field. Therefore, the dynamics of neuron i is fully determined by the parameter $\alpha_i = \epsilon k_i$ and the local mean field \bar{V}_i . The term $\epsilon k_i (\bar{V}_i - V_i)$ denotes an inhibitory feedback, which drags the action potential of neuron i to the local mean field \bar{V}_i , and α_i measures the strength of such a dragging. We note that in the BS state, all the neurons burst simultaneously from quiescent states to repetitive spikes. In the quiescent zone, $\bar{V}_i - V_i \approx 0$ and the coupling term in Eq. (3) can be neglected, we thus pay attention to \bar{V}_i in the spiking zone. An important feature in the BS state is that the spikes inside a burst are incoherent among different neurons. Therefore for a neuron with a large degree, this spike incoherence among its neighbors will result in random evolution of $\bar{V}_i(t)$. When the coupling strength is small, α_i is also small and one may, to the lowest order of approximation, neglect this ‘‘noisy’’ term and describe the dynamics of any given neuron by a perturbed system,

$$C \frac{dV}{dt} = F(V, \omega, I) - \alpha V, \quad \frac{d\omega_i}{dt} = \lambda_{\infty}(V)(\omega_{\infty}(V) - \omega), \quad (4)$$

$$\frac{dI}{dt} = -\mu \left(\frac{1}{5} + V \right).$$

The spike amplitude of such a perturbed system as the function of α is presented in Fig. 4(b), which shows a good consistency with the simulation data when α is small. When α is large, the perturbed system (4) has a little deviation from those obtained by simulation. It is reasonable that the analysis based on Eq. (4) will lose validity for large α , and the surprising linear relationship for large α observed in the simulations deserves more study and physical intuition. In short, the inhibitory coupling between neurons leads to a kind of ‘‘shrinking’’ of the spike amplitude depending on the number of its neighbors and the coupling strength.

Because of the nice linear relationship between the spike amplitude and degree, we may derive the degree distribution of the network from the distribution of the spike amplitudes. Consider a scale-free network with a power law degree distribution $p(k) \sim k^{-\gamma}$, the fraction of nodes with $k_i > k_0$ would be $P(k > k_0) = \int_{k_0}^{k_{\text{max}}} p(k) dk \approx k_0^{\gamma-1} / \gamma - 1$ given that k_{max} is large enough. According to Eq. (2), this is also the fraction of

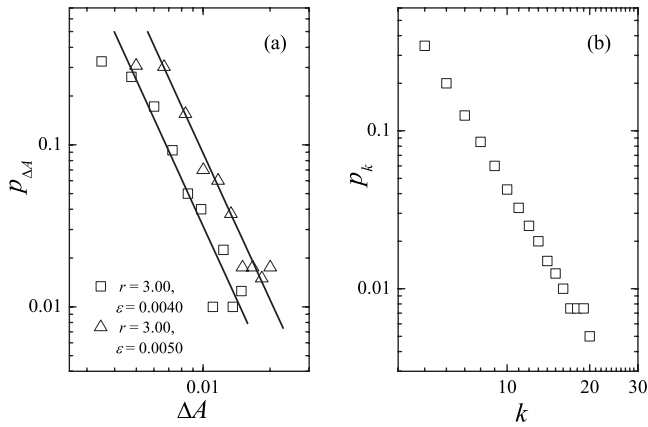


FIG. 5. Distribution of (a) ΔA for $\varepsilon=0.004$ (triangles) and $\varepsilon=0.005$ (squares) and (b) degree k on a scale-free network with $N=400$ and $\gamma=3$. The lines in (a) are used to guide the eyes and their slopes are both -3 .

nodes with spike amplitude $A_i < A_0 - c\varepsilon k_0$. It is then readily that the variable $\Delta A_i = A_0 - A_i$ also obeys the same power-law distribution as k , i.e.,

$$p(\Delta A) \sim (\Delta A)^{-\gamma}. \tag{5}$$

Therefore, by simply calculating the statistics of ΔA , we can get the scaling exponent γ .

This scheme is fairly straightforward to apply. When the system reaches the stable BS state, we just need to collect the spike amplitudes, fit the linear relationship to get A_0 , and then calculate the distribution of $\Delta A_i = A_0 - A_i$. Figure 5(a) shows the distributions of ΔA_i on a scale-free network with $N=400$ and $\gamma=3$ for $\varepsilon=0.004$ (triangle) and 0.005 (squares), and the corresponding degree distribution is shown in Fig. 5(b) for comparison. The body parts of the distribution of ΔA show rather good power law features which fit well with $p(\Delta A) \sim (\Delta A)^{-3}$ as guided by the lines. Figures 6 and 7 show more examples on scale-free networks with different scaling exponents and network size. As demonstrated, our method is able to estimate the degree distributions in a good way.

One notes that this method is not limited to scale-free networks. Actually, $p(\Delta A)$ is the same as $p(k)$ up to normal-

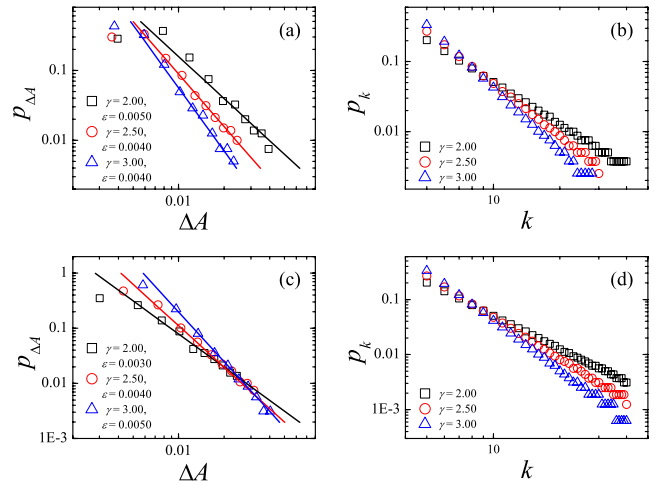


FIG. 7. (Color online) Same as Fig. 5 but for different network size N and γ . The network sizes are 800 and 1600 for (a), (b) and (c), (d), respectively. The slopes of the lines in (a) and (c) are the same as $-\gamma$.

ization. Figure 8 shows the application to two Watts–Strogatz small-world networks, constructed by randomly rewiring 10% of the edges of regular network of 400 neurons whose average degrees are 18 and 20. The left panel shows the degree distribution and the right one gives the distribution of ΔA , and the consistency is acceptable despite small quantitative discrepancies.

One may then wonder whether the method proposed above is model specific or universal. To answer this question, we have also performed similar studies on coupled HR neuron networks. We find that when the coupling is weak, BS can be observed, and the linear relationship between the spike amplitude and node degree still holds. Consequently, the degree distribution can also be easily revealed via the counting statistics of the spike amplitudes, as shown in Fig. 9 for scale-free networks with 400 HR neurons. However, when the coupling strength is strong, the linear relationship fails although BS still exists. As we already know,¹⁵ the coupled HR system may undergo a bifurcation of the bursting mechanism, from FHC type to FH type, with the increment of the coupling strength. Interestingly, we find Eq. (2)

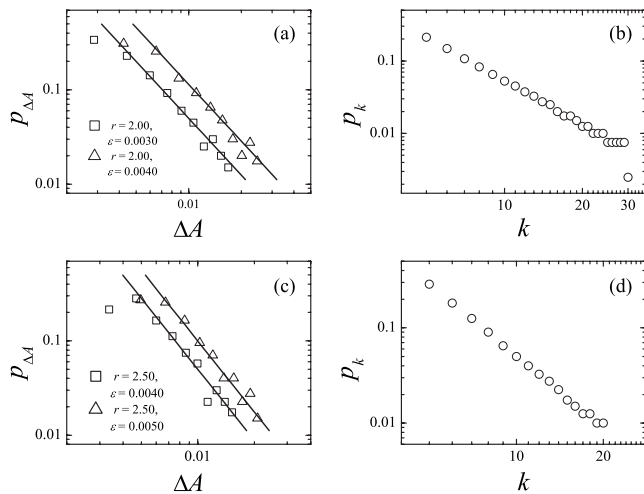


FIG. 6. Same as Fig. 5 but for different γ and ε . The slopes of the lines in (a) and (c) are the same as $-\gamma$.

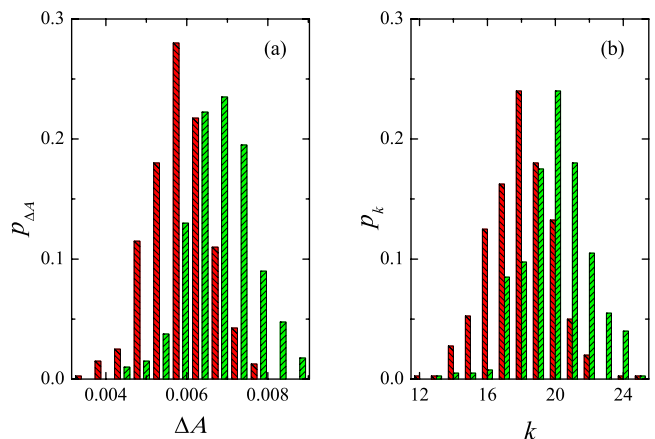


FIG. 8. (Color online) Distribution of (a) neuron degree and (b) ΔA on two small-world networks consisting of 400 nodes with average degrees 18 (backslash) and 20 (/), respectively.

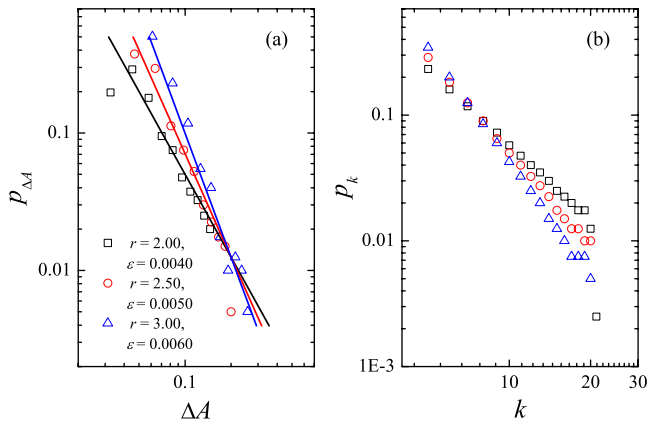


FIG. 9. (Color online) Same as Fig. 5 but for the HR neuron networks with different γ . The lines in (a) are used to guide the eyes and slopes of them are $-\gamma$.

is valid for all the neurons with FHC bursting, while it fails for neurons with FH bursting. This result indicates that it is the bursting type that determines whether our method is valid instead of the neuron model. If the bursting is FHC type, the limit cycles of the fast subsystem have a little change from fold bifurcation to homoclinic bifurcation, and the spiking amplitudes are almost the same in a burst. However, if the bursting is FH type, the limit cycles shrink to zero from fold bifurcation to Hopf bifurcation, and the spiking amplitudes are decreasing in the course of a burst. Therefore, the intraburst stationarity of spike amplitudes, which is good in FHC bursting but bad in FH bursting, is the difference between these two types of bursting. Thus we can say the spike amplitude stationarity in a burst may be the necessary condition of the linear relationship of the neurons' spiking amplitudes and the degree.

In summary, this study proposed an efficient method to estimate the degree distribution of coupled bursting neuron networks. It works based on the fact that the spike amplitude of a given neuron shows an excellently decreasingly linear relationship with its degree, when the system reaches BS. We demonstrate the validity of this scheme on scale-free as well

as small-world networks. A simple local mean field analysis shows that spike incoherence among the neurons possibly plays a key role for the linear dependence. Although we have mainly used ML model in the present work, we note that the method proposed here may also apply to other bursting neuron models of FH type. Since synchronous spike-bursting activity is of particular importance in real neuron systems, our study may find practical applications for reverse engineering the topology of neuron networks.

The work was supported by the National Science Foundation of China (Grant No. 20673106).

¹M. E. J. Newman, *Phys. Today* **61**, 33 (2008).

²R. Albert and A. L. Barabási, *Rev. Mod. Phys.* **74**, 47 (2002); S. N. Dorogovtsev and J. F. F. Mendes, *Adv. Phys.* **51**, 1079 (2002); M. E. J. Newman, *SIAM Rev.* **45**, 167 (2003); S. Boccaletti, V. Latora, Y. Moreno, M. Chavez, and D.-U. Hwang, *Phys. Rep.* **424**, 175 (2006).

³E. M. Izhikevich, *Dynamical Systems in Neuroscience: The Geometry of Excitability and Bursting* (MIT, Cambridge, MA, 2007).

⁴M. I. Rabinovich, P. Varona, A. I. Selverston, and H. D. I. Abarbanel, *Rev. Mod. Phys.* **78**, 1213 (2006).

⁵D. J. Watts and S. H. Strogatz, *Nature (London)* **393**, 440 (1998).

⁶A. L. Barabási and R. Albert, *Science* **286**, 509 (1999).

⁷A. Arenas *et al.*, *Phys. Rep.* **93**, 469 (2008); S. N. Dorogovtsev, A. V. Goltsev, and J. F. F. Mendes, *Rev. Mod. Phys.* **80**, 1275 (2008).

⁸L. M. Pecora and T. L. Carroll, *Phys. Rev. Lett.* **80**, 2109 (1998); M. Barahona and L. M. Pecora, *ibid.* **89**, 054101 (2002).

⁹R. Pastor-Satorras and A. Vespignani, *Phys. Rev. Lett.* **86**, 3200 (2001).

¹⁰F. Qi, Z. Hou, and H. Xin, *Phys. Rev. Lett.* **91**, 064102 (2003).

¹¹D. Yu, M. Righero, and L. Kocarev, *Phys. Rev. Lett.* **97**, 188701 (2006).

¹²A. Arenas, A. Díaz-Guilera, and C. J. Pérez-Vicente, *Phys. Rev. Lett.* **96**, 114102 (2006).

¹³M. Timme, *Phys. Rev. Lett.* **98**, 224101 (2007).

¹⁴S. L. Bu and I. M. Jiang, *Europhys. Lett.* **82**, 68001 (2008).

¹⁵Y. Shen, Z. Hou, and H. Xin, *Phys. Rev. E* **77**, 031920 (2008).

¹⁶E. M. Izhikevich, *Int. J. Bifurcation Chaos Appl. Sci. Eng.* **10**, 1172 (2000); *SIAM Rev.* **43**, 315 (2001).

¹⁷O. Sporns and C. J. Honey, *Proc. Natl. Acad. Sci. U.S.A.* **103**, 19219 (2006); D. S. Bassett and E. Bullmore, *Neuroscientist* **12**, 512 (2006).

¹⁸C. Morris and H. Lecar, *Biophys. J.* **35**, 193 (1981); H. Lecar, *Scholarpedia J.* **2**, 1333 (2007).

¹⁹M. Wang, Z. Hou, and H. Xin, *ChemPhysChem* **7**, 579 (2006).

²⁰M. Wang, Z. Hou, and H. Xin, *Chin. Phys.* **15**, 2553 (2006).

²¹D. Wei and X. Luo, *EPL* **78**, 68004 (2007).